

Provided for non-commercial research and education use.  
Not for reproduction, distribution or commercial use.



This article appeared in a journal published by Elsevier. The attached copy is furnished to the author for internal non-commercial research and education use, including for instruction at the authors institution and sharing with colleagues.

Other uses, including reproduction and distribution, or selling or licensing copies, or posting to personal, institutional or third party websites are prohibited.

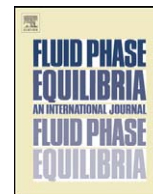
In most cases authors are permitted to post their version of the article (e.g. in Word or Tex form) to their personal website or institutional repository. Authors requiring further information regarding Elsevier's archiving and manuscript policies are encouraged to visit:

<http://www.elsevier.com/copyright>



Contents lists available at ScienceDirect

## Fluid Phase Equilibria

journal homepage: [www.elsevier.com/locate/fluid](http://www.elsevier.com/locate/fluid)

# Modeling chemical equilibria, phase behavior, and transport properties in ionic liquid systems

Peiming Wang\*, Andrzej Anderko

OLI Systems Inc., 108 American Road, Morris Plains, NJ 07950, USA

## ARTICLE INFO

## Article history:

Received 10 May 2010

Received in revised form 11 August 2010

Accepted 14 August 2010

Available online 20 August 2010

## Keywords:

Ionic liquid

Phase equilibria

Speciation

Thermodynamic properties

Transport properties

## ABSTRACT

A previously developed thermodynamic model for mixed-solvent electrolyte solutions and associated transport property models have been applied to calculating various properties of ionic liquid systems. For the analysis, imidazolium-based ionic liquids and their mixtures with water and organic solvents have been selected. The ionic liquids are treated as dissociable species that are subject to chemical speciation equilibria. The parameters of the model are determined from available thermodynamic property data including phase equilibria, activity coefficients, osmotic coefficients, enthalpies of mixing and dilution, and heat capacities. Subsequently, electrical conductivities and viscosities are calculated using the chemical speciation obtained from thermodynamic analysis. The modeling framework has been designed to reproduce the properties of ionic solutions at temperatures ranging from the freezing point to 300 °C and concentrations ranging from infinite dilution to the fused salt limit. The accuracy of the thermodynamic model has been verified by calculating vapor–liquid, liquid–liquid, and solid–liquid equilibria in wide ranges of composition and temperature. In view of the strong dependence of electrical conductivity and, secondarily, viscosity on the ionic concentration, the accurate representation of transport properties confirms that the thermodynamic speciation results are reasonable, thus verifying the applicability of the computational framework to modeling multiple thermophysical properties of ionic liquid systems.

© 2010 Elsevier B.V. All rights reserved.

## 1. Introduction

An increase in the utilization of ionic liquids (ILs) as alternative media for a more sustainable chemical industry has led to an amazing growth in research interest in such systems over the past 10 years. The characteristics that have made ionic liquids attractive to the scientific and engineering communities have been extensively reviewed [1]. Applications of ionic liquids in chemical processes require reliable and systematic information on thermodynamic and thermophysical properties including phase equilibrium behavior, activity coefficients, caloric effects, and transport properties such as viscosity and electrical and thermal conductivities. This information is of considerable importance for the proper design and selection of such systems for specific applications. In the past decade, a large amount of experimental data on ionic liquid properties has been published in the literature. An open-access, free, web-based database of physical and thermodynamic and related data has been created as a result of an IUPAC project [2]. This ionic liquids database, ILThermo, provides an extensive repository of the published experimental thermophysical, thermochemical and

transport property data for pure components, binary and ternary mixtures. These data are fundamental to a comprehensive analysis and evaluation of the thermophysical and transport properties of ionic liquids and their mixtures, thus making it possible to develop reliable thermodynamic and transport property models to be used in the analysis and simulation of chemical processes.

Phase equilibria in ionic liquids have been reproduced in the literature using classical thermodynamic models that were previously developed for nonelectrolyte systems [3]. In more recent studies using excess Gibbs energy models for electrolyte solutions, ionic liquids were assumed to be either completely dissociated to form cations and anions [4] or to be present as molecular species [5]. These models have been shown to reproduce phase equilibria with comparable results. However, among the vast published literature, there are relatively few reported studies on modeling transport properties for systems containing ionic liquids. At the same time, it is highly desirable to have a comprehensive computational framework that can be used for transport as well as thermodynamic properties. Besides its obvious practical usefulness, such a framework would provide an additional insight into the properties of ionic liquid solutions. For example, when properties relevant to transport phenomena (e.g. electrical conductivity, viscosity, and diffusivity) are of interest, the ionization behavior of ionic liquids need to be reasonably taken into account. Thus, the simultaneous representation of phase equilibria and transport

\* Corresponding author. Tel.: +1 973 539 4996; fax: +1 973 539 5922.

E-mail address: [pwang@olisystems.com](mailto:pwang@olisystems.com) (P. Wang).

properties presents a great challenge as it requires careful attention to the speciation in ionic liquid solutions.

In this study, we first apply a general, speciation-based thermodynamic model for mixed-solvent electrolyte solutions [6–8] to represent chemical and phase equilibria in selected ionic liquid systems. This model has been shown to reproduce simultaneously vapor–liquid, solid–liquid, and liquid–liquid equilibria, speciation, caloric, and volumetric properties of electrolytes in water, organic, or mixed solvents [7,8]. The model is applicable to electrolytes in the entire concentration range, i.e., from infinite dilution to the fused salt limit. In previous studies [7–9], applications of the model have been presented for completely miscible inorganic systems (e.g. acid–water mixtures), multicomponent inorganic systems containing multiple salts, acids or bases, and for systems that show complex phase behavior such as the formation of double salts, multiple hydrates, or the presence of multiple invariant points. The extensive thermodynamic property data that are available in the literature for ionic liquid systems provide an excellent opportunity to examine the applicability of this model to ionic liquids.

In the second stage, after the chemical and phase equilibria in IL systems are reproduced using the thermodynamic model, a general electrical conductivity model [10] and a viscosity model [11], both having the same range of applicability, are applied to analyze the transport properties. The calculations of electrical conductivity and viscosity in IL systems are based on speciation results obtained from the thermodynamic calculations.

The present study examines systems containing imidazolium-based ILs including pure ILs and their mixtures with water and selected organic solvents as they constitute an important class of systems for industrial applications.

## 2. Thermodynamic model

The thermodynamic model used in this study has been described in great detail in earlier papers [6,8]. The framework combines an excess Gibbs energy model for mixed-solvent electrolyte systems with a comprehensive treatment of chemical equilibria. The excess Gibbs energy is expressed as

$$\frac{G^{ex}}{RT} = \frac{G_{LR}^{ex}}{RT} + \frac{G_{II}^{ex}}{RT} + \frac{G_{SR}^{ex}}{RT} \quad (1)$$

where  $G_{LR}^{ex}$  represents the contribution of long-range electrostatic interactions,  $G_{II}^{ex}$  accounts primarily for specific ionic (ion–ion and ion–molecule) interactions and  $G_{SR}^{ex}$  is a short-range contribution resulting from intermolecular interactions. All three contributions to the excess Gibbs energy model are symmetrically normalized and are expressed in terms of mole fractions for consistency [6]. The rationale and derivation of Eq. (1) was discussed in detail by Wang et al. [6] and, therefore, only the basic features of the model are summarized here.

The long-range interaction contribution is calculated from the Pitzer–Debye–Hückel formula [6,12] expressed in terms of mole fractions and is symmetrically normalized, i.e.,

$$\frac{G_{LR}^{ex}}{RT} = - \left( \sum_i n_i \right) \frac{4A_x I_x}{\rho} \ln \left( \frac{1 + \rho I_x^{1/2}}{\sum_i x_i \left[ 1 + \rho (I_{x,i}^0)^{1/2} \right]} \right) \quad (2)$$

where the sum is over all species,  $I_x$  is the mole fraction-based ionic strength  $I_x = (1/2) \sum_i x_i z_i^2$ ,  $I_{x,i}^0$  represents the ionic strength when the system composition reduces to a pure component  $i$ , which is a hypothetical state for ions but is necessary to maintain the symmetrical normalization;  $\rho$  is related to the hard-core collision diameter

( $\rho = 14.0$ ) and  $A_x$  is given by

$$A_x = \frac{1}{3} (2\pi N_A d_s)^{1/2} \left( \frac{e^2}{4\pi \epsilon_0 \epsilon_s k_B T} \right)^{3/2} \quad (3)$$

where  $d_s$  and  $\epsilon_s$  are the molar density and the dielectric constant of the solvent, respectively. Calculation of the dielectric constant  $\epsilon_s$  in mixed solvents has been described in an earlier paper [13].

The short-range interaction contribution is calculated from the UNIQUAC equation [14]. The specific ion–interaction contribution is calculated from an ionic strength-dependent, symmetrical second virial coefficient-type expression [6]:

$$\frac{G_{II}^{ex}}{RT} = - \left( \sum_i n_i \right) \sum_i \sum_j x_i x_j B_{ij}(I_x) \quad (4)$$

where  $x_i$ ,  $x_j$  are mole fractions of species  $i$  and  $j$ , respectively;  $B_{ij}(I_x) = B_{ji}(I_x)$ ,  $B_{ii} = B_{jj} = 0$ , and the ionic strength dependence of  $B_{ij}(I_x)$  is given by

$$B_{ij}(I_x) = b_{ij} + c_{ij} \exp \left( -\sqrt{I_x + a_1} \right) \quad (5)$$

where  $b_{ij}$  and  $c_{ij}$  are adjustable parameters and  $a_1$  is set equal to 0.01. In general, the parameters  $b_{ij}$  and  $c_{ij}$  are calculated as functions of temperature as

$$b_{ij} = b_{0,ij} + b_{1,ij} T + b_{2,ij} / T \quad (6)$$

$$c_{ij} = c_{0,ij} + c_{1,ij} T + c_{2,ij} / T \quad (7)$$

For strongly dissociated electrolyte systems, the specific ion–interaction contribution,  $G_{II}^{ex}$ , is by far the most important. When associated ion pairs exist in a significant amount, or when a system involves neutral organic components, the short-range contribution,  $G_{SR}^{ex}$ , as calculated from the UNIQUAC equation, must also be introduced to account for the molecular interactions between the associated ion pairs and the solvent or between solvent components.

While the excess Gibbs energy model is used to calculate non-ideality effects on solution properties, the chemical equilibrium is governed by the chemical potentials of all species that participate in various reactions, such as ion pairing or complexation. The chemical potential of each ionic or neutral species  $i$  is determined by its standard-state contribution,  $\mu_i^0(T, P)$  and its activity coefficient,  $\gamma_i(T, P, x)$ , i.e.,

$$\mu_i(T, P, x) = \mu_i^0(T, P) + RT \ln x_i \gamma_i(T, P, x) \quad (8)$$

The standard-state chemical potentials of aqueous species,  $\mu_i^0(T, P)$ , are calculated as functions of temperature and pressure using the Helgeson–Kirkham–Flowers (HKF) equation of state [15]. Appropriate conversion must be made when combining the standard-state properties from the HKF equation of state (molality-based, infinite-dilution reference state) with the mole fraction-based and symmetrically normalized activity coefficients in order to ensure consistency for chemical equilibrium calculations [6].

For speciation calculations in non-aqueous or mixed-solvent electrolyte solutions, the chemical potential of the species is modeled by combining aqueous standard-state properties with appropriately predicted Gibbs energies of transfer. This is achieved by constraining the activity coefficient model parameters so that the Gibbs energy of transfer of ions from water to a non-aqueous solvent can be reproduced [6]. The general expression that relates the Gibbs energy of transfer to the activity coefficients is as follows:

$$\Delta_{tr} G_i^0(R \rightarrow S)_m = RT \ln \frac{\gamma_i^{*,S} \cdot M_S}{\gamma_i^{*,R} \cdot M_R} \quad (9)$$

where  $M_X$  ( $X=S$  or  $R$ ) are the molecular weights of solvent  $X$  and  $\gamma_i^{*,X}$  is the mole fraction-based unsymmetrical activity coefficient of ion  $i$  in solvent  $X$ .

### 3. Transport property models

#### 3.1. Electrical conductivity model

The model for calculating the electrical conductivity of aqueous and mixed-solvent electrolyte solutions has been described previously [10,16]. It consists of a correlation for calculating ionic conductivities at infinite dilution as a function of solvent composition and a method for predicting the effect of finite electrolyte concentration. The effect of electrolyte concentration is calculated using an extended form of the mean-spherical-approximation (MSA) theory coupled with a mixing rule for predicting the conductivity of multicomponent systems on the basis of conductivities of constituent binary cation–anion subsystems. The MSA theory has been extended to very concentrated [10,16] and mixed-solvent systems [10] by introducing effective ionic diameters that take into account various interactions between ions, solvent molecules and ion pairs. The electrical conductivity model has been coupled with thermodynamic equilibrium computations to provide the necessary concentrations of individual ions in complex, multicomponent systems.

#### 3.2. Viscosity model

The details of a viscosity model for concentrated aqueous and mixed-solvent electrolyte solutions have been described in a previous paper [11]. The model consists of two distinct parts: a mixing rule for calculating the viscosity of solvent mixtures as a function of temperature and solvent composition using viscosities and liquid molar volumes of pure components, and a model for predicting the effect of finite electrolyte concentrations. The electrolyte effect on the concentration dependence of viscosity consists of a long-range electrostatic term obtained from the Onsager–Fuoss theory, a contribution of individual ions characterized by the Jones–Dole  $B$  coefficients; and a contribution of specific interactions between ions or neutral species. Formulations for the individual ion contribution and the species interactions term have been developed to account for the effects of multiple solvents and are functions of solvent composition. The contribution of specific interactions between species is also a function of the ionic strength. As in the electrical conductivity model, the speciation that is necessary for viscosity calculations is provided by the thermodynamic equilibrium model. This makes it possible to reproduce the effects of complexation or other reactions in the solution. The model has been shown to be accurate for reproducing viscosities over wide ranges of composition with respect to both solvents and electrolytes.

In the present work, the electrical conductivity model and the viscosity model have been applied to ionic liquid systems including pure ILs and mixtures of ILs with water or organic solvents.

### 4. Challenges in modeling ionic liquids

Due to the inherent physical complexity of ionic liquids and their mixtures, the development of thermophysical models for such systems presents substantial challenges that can be summarized as follows:

1. Some ionic liquids show limited miscibility with water and organic solvents. For many immiscible systems, the liquid–liquid equilibrium binodal curve on a  $T-x$  plot is unsymmetrical due to an appreciable solubility of the molecular solvent in the IL but

a low solubility of the IL in the molecular solvent. For instance, in the BMIM-BF<sub>4</sub> + H<sub>2</sub>O mixture, the critical point is located at  $T_c$  of  $\sim 5^\circ\text{C}$  at  $x(\text{IL})$  of  $\sim 0.08$ . It is typically difficult to model phase equilibria in systems with highly unsymmetrical miscibility gaps.

2. Although the vapor pressures of pure ILs are extremely low, they are measurable and experimentally determined values have been reported [17,18]. A previously widely accepted defining characteristic of ionic liquids was their lack of volatility, which implied exerting no measurable vapor pressure and hence being non-distillable. This assumption has been demonstrated to be unfounded [19]. The vaporization of ionic liquids at low pressure followed by condensation at lower temperatures allows the separation of ionic liquid mixtures by distillation [19]. Vapor pressure data for pure ILs are needed for comprehensive modeling phase equilibria of IL systems. Additionally, due to the low volatility of ionic liquids, there is a lack of literature data for the standard-state properties (i.e., Gibbs free energy of formation  $\Delta G_f^0$ , enthalpy of formation  $\Delta H_f^0$  and entropy  $S^0$ ) for the ILs in the gas phase. This poses a challenge in modeling the thermodynamics of IL systems in the vapor–liquid equilibrium region.
3. Chemical speciation in pure ionic liquids and their mixtures with molecular solvents remains obscure, in spite of reported experimental evidence for ion association [20,21]. The ion association behavior of ILs has been a subject of debate in the literature [22]. Electrical conductivity data indicate strong ion dissociation with an ionic conductivity level comparable to that in some electrolyte solutions used in electrochemistry [22]. Meanwhile, Tokuda et al. [21,23,24] estimated IL's dissociation degree by using the molar conductivity ratio ( $\Lambda_{\text{imp}}/\Lambda_{\text{NMR}}$ ) where  $\Lambda_{\text{imp}}$  is the molar conductivity obtained by the electrochemical impedance measurements and  $\Lambda_{\text{NMR}}$  is that estimated from spin-echo NMR ionic self-diffusivity measurements through the Nernst–Einstein relation [21]. In this approach, the IL is completely dissociated if  $\Lambda_{\text{imp}}/\Lambda_{\text{NMR}} = 1$ . The obtained ratios of  $\Lambda_{\text{imp}}/\Lambda_{\text{NMR}}$  are  $\sim 0.5$ – $0.75$  for pure ILs, indicating that not all of the diffusive species contribute to the ionic conduction, i.e., there is a substantial amount of associated or aggregated ions in the systems. Another literature indication of ion association in IL systems is the result reported by Hunger et al. [20], who inferred from measured dielectric spectra that an IL was a strongly associated electrolyte at high dilution ( $X(\text{IL}) < 0.3$ ) in dichloromethane. These literature results provide qualitative information that can be useful, but are insufficient to elaborate the chemical speciation in ILs. In addition, when treating ILs as speciated systems, the standard-state thermochemical properties (i.e.,  $\Delta G_f^0$ ,  $\Delta H_f^0$  and  $S^0$ ) of these species are needed. These data are usually not available in the literature. The lack of speciation data and thermochemical properties for the speciated ionic liquids poses a great challenge in modeling such systems.

In addition to these difficulties, the traditional approaches used for calculating thermodynamic parameters for organic components in the mixed-solvent electrolyte framework [6] are not directly applicable to ILs due to their “ionic” features, even though the ILs exist in the pure liquid state like the organic solvents. Therefore, a different approach must be used for parameterizing such systems.

### 5. Approach to modeling ionic liquids

Based on the literature information and the available thermo-physical property data and taking into consideration the specific characteristics of the ILs, the most appropriate approach is to treat the ILs as highly dissociable species with speciation equilibria that lead to the formation of associated ion pairs. The ion association patterns vary with the system's conditions (i.e., concen-

tration and temperature). In the context of this paper, “association” or “ion association” indicates the formation of the IL ion pairs as opposed to the ion dissociation of the ILs. The equilibrium conditions and standard-state thermochemical properties for associated ion pairs in the liquid phase are determined together with the thermochemical properties of gaseous IL molecules using available thermodynamic data for pure ILs and mixtures of ILs with non-ILs. The input data include (1) vapor pressure, (2) liquid–liquid equilibria, (3) solid–liquid equilibria, (4) osmotic coefficients, (5) activity coefficients for non-IL components at infinite dilution, (6) heats of mixing and of dilution, and (7) heat capacities. In this approach, the calculated Gibbs energy, enthalpy, and heat capacity of the ILs are constructed from contributions of dissociated ions, associated ion pairs and undissociated molecules.

The vapor–liquid equilibrium, liquid–liquid equilibrium, activity and osmotic coefficient data directly constrain the excess Gibbs energy whereas the solid–liquid equilibrium data can be used to constrain both the excess Gibbs energy and the properties of the solid phases that are in equilibrium with the liquid phase. Constraining the excess Gibbs energy using vapor–liquid and solid–liquid equilibrium data in the thermodynamic modeling also makes it possible to determine the standard-state properties (i.e., Gibbs free energy of formation  $\Delta G_f^0$ , enthalpy of formation  $\Delta H_f^0$  and entropy  $S^0$ ) for the gaseous and solid IL phases, for which no literature data have been found.

While a single type of data can be used alone to determine the model parameters and represent the experimental results, the use of multiple data types is advisable to ensure the accuracy and consistency of model parameters. For example, caloric data (heat of mixing or dilution and heat capacities) are useful to determine the temperature dependence of model parameters. This makes it possible to make reliable predictions of solubilities well beyond the temperature range of experimental solubility data. The predictive features of the thermodynamic model have been investigated and demonstrated in earlier studies [8,25] where the predicted chemical speciation results were found in remarkable agreement with literature data for a highly associated electrolyte system using thermodynamic model parameters developed based on the activity, phase equilibrium and caloric data [8], and the solubility in multicomponent systems (beyond ternary) has been accurately predicted using the parameters based on constituent binary and ternary subsystems [25].

The chemical speciation results obtained from the thermodynamic model are then used in the transport property models in the determination of model parameters for calculating the solution conductivities and viscosities. As the electrical conductivity is an important indirect measure of the degree of association in ionic solutions, the results of electrical conductivity calculations can indicate the appropriateness and accuracy of the chemical speciation as predicted by the thermodynamic model.

## 6. Results and discussion

The present study examines systems containing imidazolium-based ILs including pure ILs and their mixtures with water and selected organic components. These systems have been extensively studied in the literature and an appreciable amount of experimental data is available.

The mixtures of ILs with water and the corresponding pure ILs are examined together to determine the standard-state thermochemical properties ( $\Delta G_f^0$ ,  $\Delta H_f^0$ ,  $S^0$ ) for the gaseous molecules, associated ion pairs, and solid phases, whichever applies, together with ion–interaction parameters that are specific to the systems examined. The model is then applied to the mixtures of ILs with organic components to determine the appropriate inter-

**Table 1**  
Thermodynamic model parameters for the EMIM-PF<sub>6</sub> + water and EMIM-PF<sub>6</sub> + toluene systems.

Parameters	System, types of data, temperature range, references
Binary interaction parameters <sup>a,b</sup> $b_0(\text{EMIM}^+, \text{EMIM}\cdot\text{PF}_6^0) = b_0(\text{PF}_6^-, \text{EMIM}\cdot\text{PF}_6^0) = 7.82211$	EMIM-PF <sub>6</sub> <sup>0</sup> + H <sub>2</sub> O, LLE, SLE, Cp, T = 35–180 °C, Refs. [26,32]
$b_1(\text{EMIM}^+, \text{EMIM}\cdot\text{PF}_6^0) = b_1(\text{PF}_6^-, \text{EMIM}\cdot\text{PF}_6^0) = 8.22740\text{E}-03$ $c_0(\text{EMIM}^+, \text{EMIM}\cdot\text{PF}_6^0) = c_0(\text{PF}_6^-, \text{EMIM}\cdot\text{PF}_6^0) = -8.78837$ $a_0(\text{H}_2\text{O}, \text{EMIM}\cdot\text{PF}_6^0) = 1894.57$ $a_0(\text{EMIM}\cdot\text{PF}_6^0, \text{H}_2\text{O}) = 1683.79$ $a_1(\text{H}_2\text{O}, \text{EMIM}\cdot\text{PF}_6^0) = -1.13465$ $a_1(\text{EMIM}\cdot\text{PF}_6^0, \text{H}_2\text{O}) = 0.326072$	
UNIQUAC structural parameters for aqueous species EMIM-PF <sub>6</sub> (aq): R = 5.094, Q = 5.284 EMIM <sup>+</sup> : R = 4.158, Q = 2.198 PF <sub>6</sub> <sup>-</sup> : R = 0.92, Q = 1.4 <sup>c</sup>	
Parameters for aqueous and solid species <sup>d</sup> EMIM-PF <sub>6</sub> (aq): $\Delta G_f^0 = -1879.23$ , $S^0 = 474.713$ EMIM <sup>+</sup> : $\Delta G_f^0 = -5.734$ , $S^0 = 71.779$ PF <sub>6</sub> <sup>-</sup> : $\Delta G_f^0 = -1843.26$ , $S^0 = 167.360^e$ EMIM-PF <sub>6</sub> (s): $\Delta G_f^0 = -1884.76$ , $S^0 = 390.516$	
Binary interaction parameters <sup>a,b</sup> $b_0(\text{EMIM}\cdot\text{PF}_6^0, \text{toluene}) = 2.04289\text{E}-02$	EMIM-PF <sub>6</sub> <sup>0</sup> + toluene, LLE and SLE, T = 48–105 °C, Ref. [27]
$c_0(\text{EMIM}\cdot\text{PF}_6^0, \text{toluene}) = 2.00689\text{E}-02$ $b_0(\text{EMIM}^+, \text{toluene}) = b_0(\text{PF}_6^-, \text{toluene}) = 9.61760\text{E}-02$ $b_1(\text{EMIM}^+, \text{toluene}) = b_1(\text{PF}_6^-, \text{toluene}) = 1.10002\text{E}-03$ $a_0(\text{toluene}, \text{EMIM}\cdot\text{PF}_6^0) = 2369.19$ $a_0(\text{EMIM}\cdot\text{PF}_6^0, \text{toluene}) = -829.396$	

<sup>a</sup> Parameters not listed are set equal to zero. All parameters are determined in this study unless otherwise noted.

<sup>b</sup>  $b$  and  $c$ 's are parameters in Eqs. (5)–(7),  $a$ 's are those of UNIQUAC (Ref. [6], Eqs. (10)–(15) and Eq. (34)).

<sup>c</sup> Values for inorganic ions are assigned the same values as those for water [14].

<sup>d</sup> Units are in kJ mol<sup>-1</sup> for  $\Delta G_f^0$ , J mol<sup>-1</sup> K<sup>-1</sup> for  $S^0$ .

<sup>e</sup> Values determined from a previous study [10].

action parameters that give the best fit to the experimental thermodynamic data. For example, when working with EMIM-PF<sub>6</sub> (1-ethyl-3-methyl-imidazolium hexafluorophosphate), thermochemical properties for the associated ion pair, EMIM-PF<sub>6</sub>(aq) and solid EMIM-PF<sub>6</sub>(s) can be determined, together with binary interaction parameters for EMIM-PF<sub>6</sub>(aq)/H<sub>2</sub>O, EMIM-PF<sub>6</sub>(aq)/EMIM<sup>+</sup>, and EMIM-PF<sub>6</sub>(aq)/PF<sub>6</sub><sup>-</sup>, using experimental thermodynamic data for the pure ionic liquid EMIM-PF<sub>6</sub> and mixtures of EMIM-PF<sub>6</sub> + water, including liquid–liquid and solid–liquid equilibrium data, and heat capacities (cf., Table 1). The literature information on the ion association degree [20,21] is also considered, but is used only as a qualitative guide in determining the chemical speciation, and most importantly in obtaining the best fit to the more reliable experimental thermodynamic data. The mixtures of EMIM-PF<sub>6</sub> with toluene or with other organic components are examined after the aqueous IL system has been analyzed and relevant parameters have been determined. Thus, based on EMIM-PF<sub>6</sub> + toluene data, binary interaction parameters such as EMIM-PF<sub>6</sub>(aq)/toluene, toluene/EMIM<sup>+</sup>, and toluene/PF<sub>6</sub><sup>-</sup> are derived (Table 1). It has been found that a better fit to the experimental data can be obtained if the UNIQUAC surface and size parameters for the associated ion pair, as well as the bulky cations or anions, are treated as adjustable parameters. However, once determined, these parameters must remain the same for all systems, pure or mixed, in which they exist. The results of phase equilibrium computations for

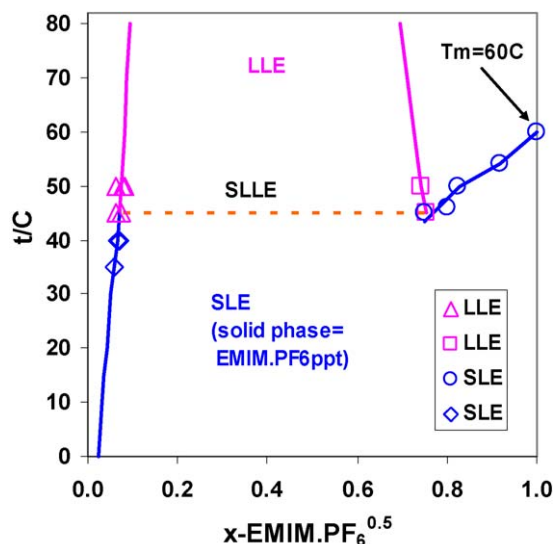


Fig. 1. Calculated and experimental phase equilibria for the water + EMIM-PF<sub>6</sub> system. Experimental data are from Wong et al. [26].

the EMIM-PF<sub>6</sub> + water and EMIM-PF<sub>6</sub> + toluene systems are shown in Figs. 1 and 2, respectively [26,27]. The corresponding model parameters are summarized in Table 1, which also lists the literature information that has been used in the determination of these parameters in each system. In both cases, the liquid–liquid equilibria and solid–liquid equilibria are simultaneously represented with good accuracy all the way to the limit of the melting temperature of the pure ionic liquid (~60 °C). The *x*-axes in these figures show the square root of the mole fraction of the ionic liquid,  $x(\text{EMIM}\cdot\text{PF}_6)$  to better visualize the range of low ionic liquid concentrations (Fig. 1) because the miscibility gaps in these systems are asymmetrical with very low solubilities of EMIM-PF<sub>6</sub> in molecular solvents and appreciable solubilities of the non-ionic components in the ILs.

Fig. 3 shows the results of calculating activity coefficients of molecular solutes (e.g. water, hexane, and methanol) at infinite dilution in ILs,  $\gamma_i^\infty$ . Such information is of most interest for solvent extraction and extractive distillation, as the value of  $\gamma_i^\infty$  provides a measure of the potential of an IL for separating organic mixtures of distinctive components (e.g. aromatic/aliphatic, polar/non-polar)

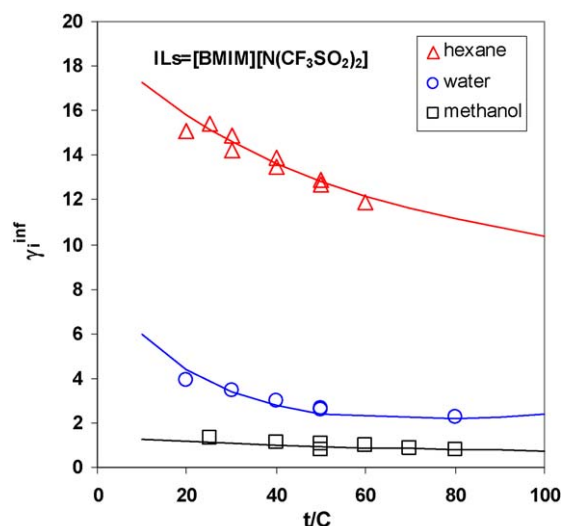


Fig. 3. Calculated and experimental activity coefficients of hexane, water, and methanol at infinite dilution in BMIM-N(CF<sub>3</sub>SO<sub>2</sub>)<sub>2</sub>. Experimental data are from Krummen et al. [28], Heintz et al. [29], Zhang et al. [30], and Kato and Gmehling [31].

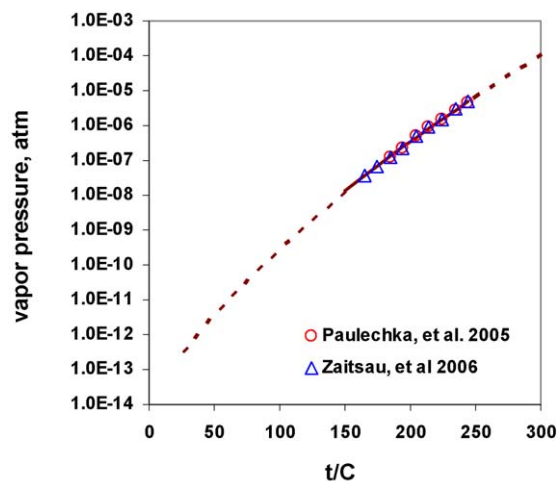


Fig. 4. Calculated and experimental vapor pressure over pure liquid BMIM-N(CF<sub>3</sub>SO<sub>2</sub>)<sub>2</sub> as a function of temperature. Experimental data are from Zaitsau et al. [17] and Paulechka et al. [18]. Dashed lines are extrapolated using the model.

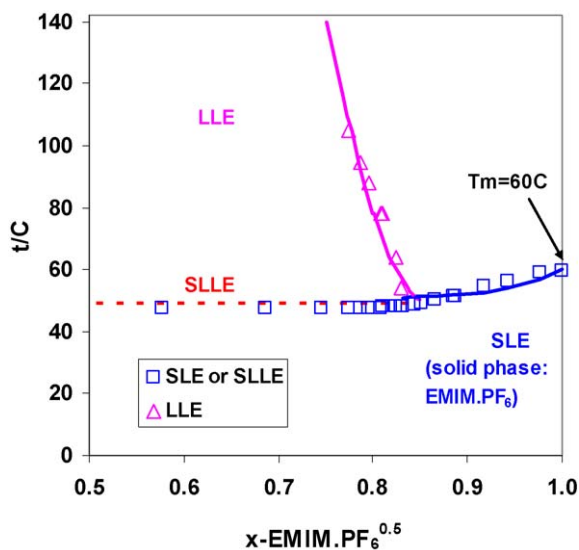


Fig. 2. Calculated and experimental phase equilibria for the toluene + EMIM-PF<sub>6</sub> system. Experimental data are from Domanska and Marciniak [27].

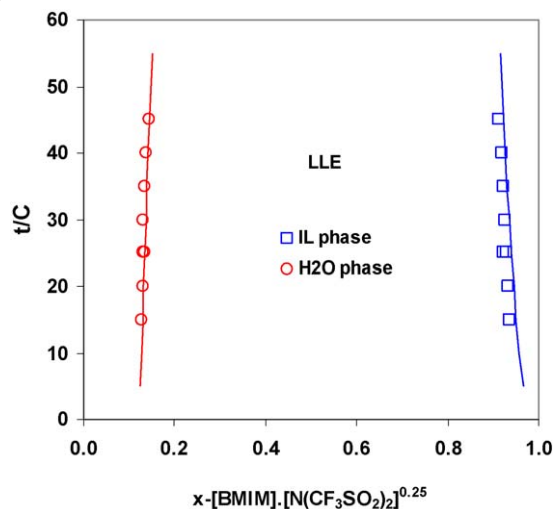
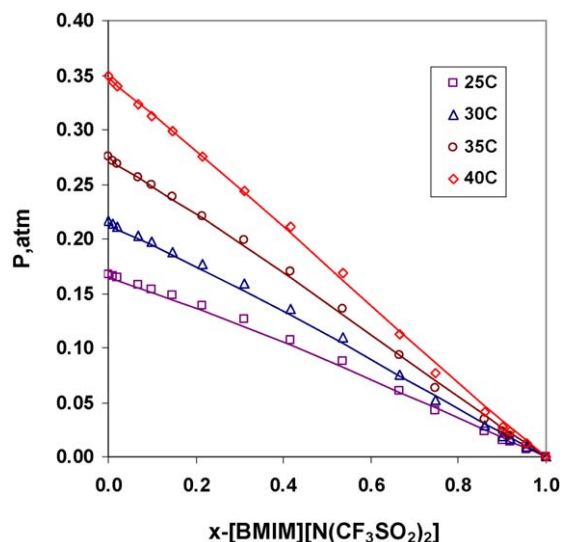


Fig. 5. Calculated and experimental liquid–liquid equilibria in the BMIM-N(CF<sub>3</sub>SO<sub>2</sub>)<sub>2</sub> + water system. Experimental data are from Freire et al. [33].



**Fig. 6.** Calculated and experimental vapor–liquid equilibria for the  $\text{BMIM}\cdot\text{N}(\text{CF}_3\text{SO}_2)_2$  + methanol system as a function of  $x_{\text{BMIM}\cdot\text{N}(\text{CF}_3\text{SO}_2)_2}$  at various temperatures. Experimental data are from Verevkin et al. [35].

and can be used to quantify the volatility of the solute as well as to provide information about intermolecular energy between solvent and solute [3,28–31]. Accurate prediction of the activity coefficients of molecular solutes at infinite dilution in ILs as shown in Fig. 3 indicates that the model can be used for selecting effective extraction fluids.

To perform a comprehensive analysis of multiple thermophysical properties, systems containing 1-butyl-3-methylimidazolium bis[(trifluoromethyl)sulfonyl]imide ( $\text{BMIM}\cdot\text{N}(\text{CF}_3\text{SO}_2)_2$ ) have been selected. For these systems, the available thermodynamic data include the vapor pressure, heat capacity, and density of the pure ionic liquid as a function of temperature [32], liquid–liquid equilibria in the  $\text{BMIM}\cdot\text{N}(\text{CF}_3\text{SO}_2)_2$  + water system [33], vapor–liquid equilibria in the mixtures of  $\text{BMIM}\cdot\text{N}(\text{CF}_3\text{SO}_2)_2$  with water [31,34] and with methanol [35], activity coefficients of molecular solutes (water, methanol, hexane, and toluene) at infinite dilution in the

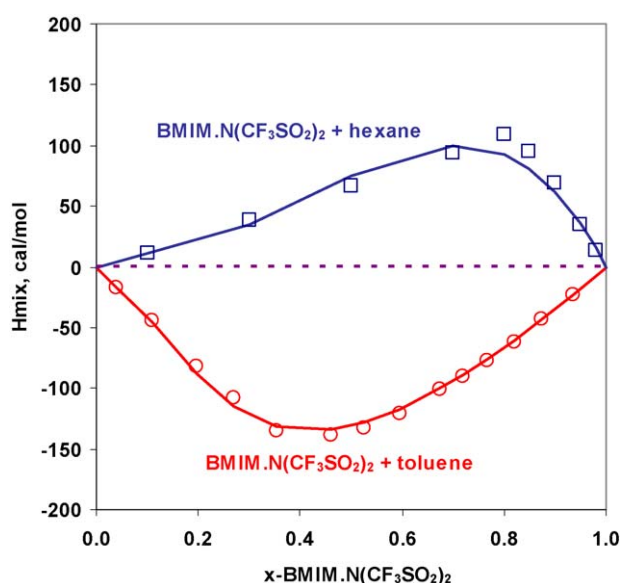


**Fig. 7.** Calculated and experimental heats of mixing for  $\text{BMIM}\cdot\text{N}(\text{CF}_3\text{SO}_2)_2$  + hexane and  $\text{BMIM}\cdot\text{N}(\text{CF}_3\text{SO}_2)_2$  + toluene as a function of  $x_{\text{BMIM}\cdot\text{N}(\text{CF}_3\text{SO}_2)_2}$  at 90 °C. Experimental data are from Nebig et al. [36].

**Table 2**

Thermodynamic model parameters for the binary systems of  $\text{BMIM}\cdot\text{N}(\text{CF}_3\text{SO}_2)_2$  with water, hexane, toluene, and methanol.

Parameters	Systems
UNIQUAC structural parameters $\text{BMIM}\cdot\text{N}(\text{CF}_3\text{SO}_2)_2(\text{aq}): R = 16.33, Q = 11.39$ $\text{N}(\text{CF}_3\text{SO}_2)_2^-: R = 6.817, Q = 4.444$ $\text{BMIM}^+: R = 10.12, Q = 6.718$ Parameters for aqueous and gaseous species <sup>a</sup> $\text{BMIM}\cdot\text{N}(\text{CF}_3\text{SO}_2)_2(\text{aq}): \Delta G_f^0 = -32.6632,$ $S^0 = 312.956$	$\text{BMIM}\cdot\text{N}(\text{CF}_3\text{SO}_2)_2 + \text{H}_2\text{O}$ . Types of data: VLE, LLE, $\gamma_{\text{H}_2\text{O}}^{\text{inf}}$ , Cp. $T = -3\text{--}244$ °C. Refs. [17,18,28,30,31,33,34,45]
$\text{BMIM}^+$ and $\text{N}(\text{CF}_3\text{SO}_2)_2^-: \Delta G_f^0 = -5.0422,$ $S^0 = 119.451$ $\text{BMIM}\cdot\text{N}(\text{CF}_3\text{SO}_2)_2(\text{g}): \Delta G_f^0 = 28.7121,$ $S^0 = 318.117$ Binary interaction parameters <sup>b</sup> $b_0(\text{BMIM}\cdot\text{N}(\text{CF}_3\text{SO}_2)_2^0, \text{H}_2\text{O}) = -13.9364$ $b_1(\text{BMIM}\cdot\text{N}(\text{CF}_3\text{SO}_2)_2^0, \text{H}_2\text{O}) = 1.51252\text{E}-03$ $b_2(\text{BMIM}\cdot\text{N}(\text{CF}_3\text{SO}_2)_2^0, \text{H}_2\text{O}) = -1160.16$ $a_0(\text{BMIM}\cdot\text{N}(\text{CF}_3\text{SO}_2)_2^0, \text{H}_2\text{O}) = -427.462$ $a_1(\text{BMIM}\cdot\text{N}(\text{CF}_3\text{SO}_2)_2^0, \text{H}_2\text{O}) = -24.7736$	
$b_0(\text{N}(\text{CF}_3\text{SO}_2)_2^-, \text{hexane})^c = -4.67660$	$\text{BMIM}\cdot\text{N}(\text{CF}_3\text{SO}_2)_2 + \text{hexane}$ . Types of data: VLE, $\gamma_{\text{hexane}}^{\text{inf}}$ , Hmix. $T = 20\text{--}90$ °C. Refs. [28,29,36,46]
$b_1(\text{N}(\text{CF}_3\text{SO}_2)_2^-, \text{hexane})^c = -5.15968\text{E}-03$ $b_0(\text{BMIM}^+, \text{hexane}) = -0.407765$ $b_1(\text{BMIM}^+, \text{hexane}) = 1.73161\text{E}-02$ $a_0(\text{BMIM}\cdot\text{N}(\text{CF}_3\text{SO}_2)_2^0, \text{hexane}) = 3605.66$ $a_1(\text{BMIM}\cdot\text{N}(\text{CF}_3\text{SO}_2)_2^0, \text{hexane}) = -0.241949$ $a_0(\text{hexane}, \text{BMIM}\cdot\text{N}(\text{CF}_3\text{SO}_2)_2^0) = -1435.83$ $a_1(\text{hexane}, \text{BMIM}\cdot\text{N}(\text{CF}_3\text{SO}_2)_2^0) = 0.903284$	
$a_0(\text{methanol}, \text{BMIM}\cdot\text{N}(\text{CF}_3\text{SO}_2)_2^0) = 2488.01$	$\text{BMIM}\cdot\text{N}(\text{CF}_3\text{SO}_2)_2 + \text{methanol}$ . Types of data: VLE, $\gamma_{\text{methanol}}^{\text{inf}}$ . $T = 25\text{--}80$ °C. Refs. [29,35]
$a_1(\text{methanol}, \text{BMIM}\cdot\text{N}(\text{CF}_3\text{SO}_2)_2^0) = -9.62270$ $a_0(\text{BMIM}\cdot\text{N}(\text{CF}_3\text{SO}_2)_2^0, \text{methanol}) = 1686.84$ $a_1(\text{BMIM}\cdot\text{N}(\text{CF}_3\text{SO}_2)_2^0, \text{methanol}) = 3.03101$ $b_0(\text{BMIM}^+, \text{toluene})^c = 5.21751$	$\text{BMIM}\cdot\text{N}(\text{CF}_3\text{SO}_2)_2 + \text{toluene}$ . Types of data: VLE, $\gamma_{\text{toluene}}^{\text{inf}}$ , Hmix. Refs. [28–30,36,46]
$b_1(\text{BMIM}^+, \text{toluene})^c = -2.20016\text{E}-02$ $b_0(\text{N}(\text{CF}_3\text{SO}_2)_2^-, \text{toluene})^c = -7.78556$ $b_1(\text{N}(\text{CF}_3\text{SO}_2)_2^-, \text{toluene})^c = 2.96765\text{E}-02$ $a_0(\text{toluene}, \text{BMIM}\cdot\text{N}(\text{CF}_3\text{SO}_2)_2^0) = 4914.48$ $a_1(\text{toluene}, \text{BMIM}\cdot\text{N}(\text{CF}_3\text{SO}_2)_2^0) = -1.73757$ $a_0(\text{BMIM}\cdot\text{N}(\text{CF}_3\text{SO}_2)_2^0, \text{toluene}) = -1678.36$ $a_1(\text{BMIM}\cdot\text{N}(\text{CF}_3\text{SO}_2)_2^0, \text{toluene}) = 1.02546$	

<sup>a</sup> Units are in  $\text{kJ mol}^{-1}$  for  $\Delta G_f^0$ ,  $\text{J mol}^{-1} \text{K}^{-1}$  for  $S^0$ .

<sup>b</sup> See footnotes a and b in Table 1.

<sup>c</sup> Parameters determined to apply to other systems as well: e.g.  $\text{BMIM}\cdot\text{PF}_6 + \text{toluene}$  ( $\text{BMIM}^+, \text{toluene}$ ),  $\text{EMIM}\cdot\text{N}(\text{CF}_3\text{SO}_2)_2 + \text{toluene}$  ( $\text{N}(\text{CF}_3\text{SO}_2)_2^-, \text{toluene}$ ),  $\text{EMIM}\cdot\text{N}(\text{CF}_3\text{SO}_2)_2 + \text{hexane}$  ( $\text{N}(\text{CF}_3\text{SO}_2)_2^-, \text{hexane}$ ).

ionic liquid [28–31], and heats of mixing of  $\text{BMIM}\cdot\text{N}(\text{CF}_3\text{SO}_2)_2$  with toluene and with hexane [36]. Selected results for these thermodynamic properties are shown in Figs. 3–7. Thus, various types of experimental data have been accurately reproduced by a consistent set of model parameters, which are listed in Table 2, together with literature sources from which these parameters were developed. The experimental data and the model results indicate that  $\text{BMIM}\cdot\text{N}(\text{CF}_3\text{SO}_2)_2$  is immiscible with water, with a miscibility gap as shown in Fig. 5, but can be fully miscible with organic solvents

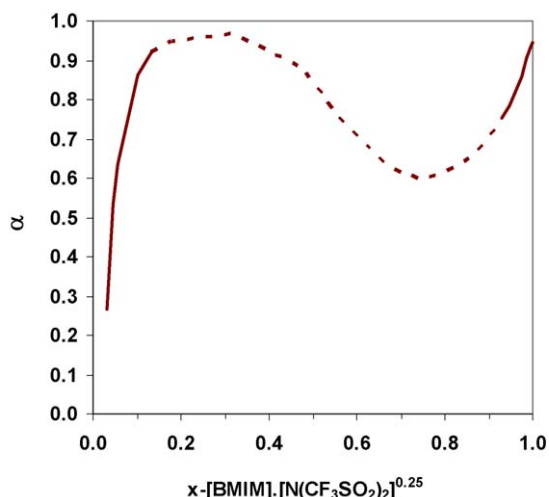


Fig. 8. Predicted association degree,  $\alpha$ , in the mixtures of BMIM-N(CF<sub>3</sub>SO<sub>2</sub>)<sub>2</sub> + water at 25 °C as a function of  $x_{\text{BMIM-N(CF}_3\text{SO}_2)_2}^{0.25}$ . Results represented by the dashed line are obtained assuming no miscibility gap.

such as hexane, toluene, and methanol under the conditions of the experimental measurements. Specifically, the vapor pressure and heat of mixing data have been measured in the entire composition range for the mixtures without any indication of a miscibility gap, as shown in Figs. 6 and 7. The thermodynamic model predicts the speciation both in the pure ionic liquid at varying temperatures and in the mixtures of ILs with other components at varying compositions. Fig. 8 shows the predicted degree of association,  $\alpha$ , of the ionic liquid as defined by  $\alpha = x_{\text{BMIM-N(CF}_3\text{SO}_2)_2(\text{AQ})} / (x_{\text{BMIM-N(CF}_3\text{SO}_2)_2(\text{AQ})} + x_{\text{BMIM}^+})$  in the mixtures of BMIM-N(CF<sub>3</sub>SO<sub>2</sub>)<sub>2</sub> + water as a function of the mole fraction of the ionic liquid. The same quantity is shown in Fig. 9 in a pure ionic liquid and for a fixed liquid phase composition  $x_{\text{BMIM-N(CF}_3\text{SO}_2)_2} = 0.9$ . The model predicts a drastically increased association degree as the ionic liquid mole fraction increases in both the water-dominated and IL-dominated liquid phases (Fig. 8). It is interesting to note that this predicted association trend resembles that observed in highly speciated electrolyte systems such as aqueous sulfuric acid solutions [8], thus indicating an electrolyte nature with a strong association tendency in the ionic liquid systems. This result is qualitatively consistent with what is indicated by the measurements of Hunger et al. [20] and Tokuda et al. [21]. In the pure

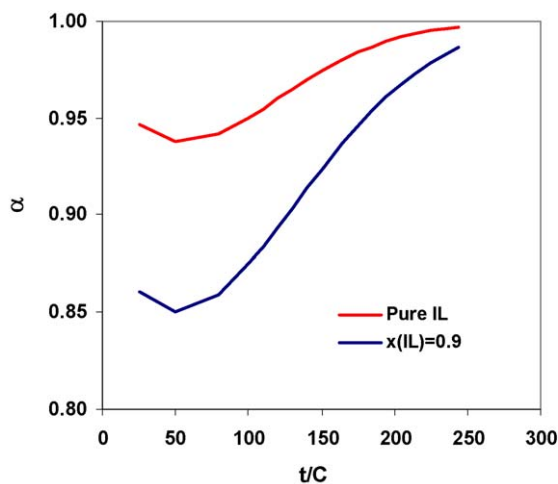


Fig. 9. Predicted association degree,  $\alpha$ , as a function of temperature in pure liquid BMIM-N(CF<sub>3</sub>SO<sub>2</sub>)<sub>2</sub> (upper line) and in the mixture of BMIM-N(CF<sub>3</sub>SO<sub>2</sub>)<sub>2</sub> ( $x=0.9$ ) + water ( $x=0.1$ ).

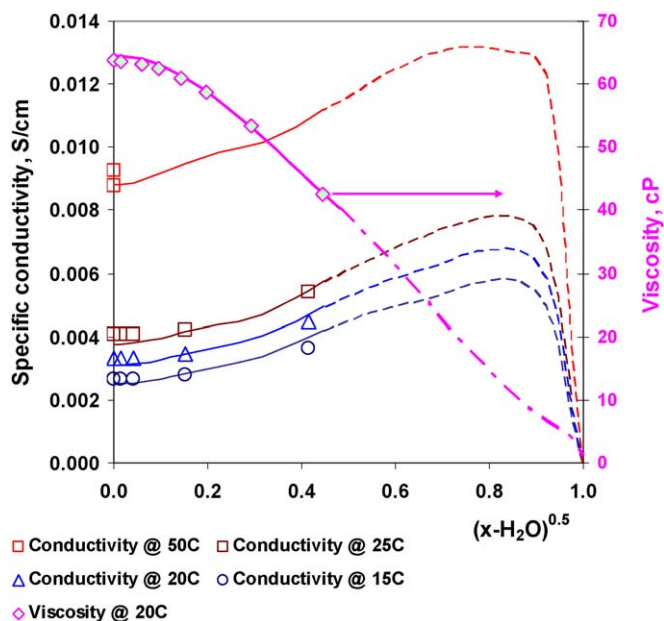


Fig. 10. Calculated and experimental specific conductivity and viscosity of BMIM-N(CF<sub>3</sub>SO<sub>2</sub>)<sub>2</sub> + water mixtures at various temperatures as a function of  $x_{\text{H}_2\text{O}}^{0.5}$ . Experimental data are from Widegren et al. [42,43]. Dashed lines are the hypothetical results in the absence of phase splitting.

ionic liquid and in aqueous mixtures containing 90% of the ionic liquid, the association degree is predicted to decrease with temperature below  $\sim 50$  °C, and increase with temperature at  $T > 50$  °C. The increase in association with temperature has been observed for many associating electrolytes [37–39], and is consistent with the Bjerrum association theory [40] in which the Bjerrum electrostatic distance ( $q_{ij} = |z_i z_j| e^2 / (2\epsilon kT)$ ) increases with temperature, due to a decrease in the product of the dielectric constant ( $\epsilon$ ) and temperature ( $T$ ). This indicates an increased formation of ion pairs at higher temperatures [41]. The change in the trend of association with temperature at  $\sim 50$  °C may be caused by a change in the intermolecular interactions (e.g. H-bonding) that can be highly directional in the short range due to the bulky ionic size and asymmetrical charge distribution [22], which may change with temperature.

The speciation results predicted by the thermodynamic model provide a basis for a consistent treatment of transport properties in ionic liquid systems, as these properties are highly depen-

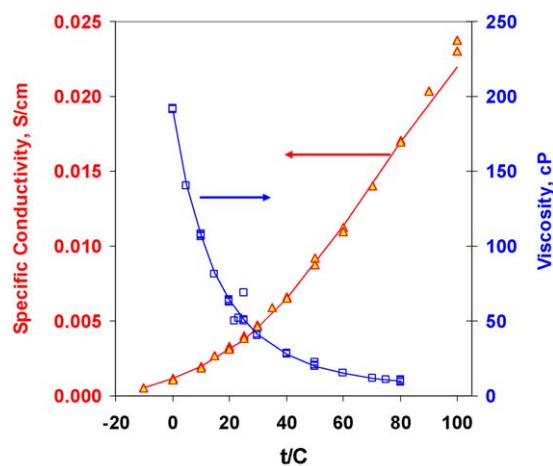


Fig. 11. Calculated and experimental specific conductivity and viscosity of the pure ionic liquid BMIM-N(CF<sub>3</sub>SO<sub>2</sub>)<sub>2</sub> as a function of temperature. Experimental data are from Tokuda et al. [21,24], Widegren et al. [42], and Harris et al. [44].



**Table 3**  
Electrical conductivity and viscosity model parameters for the EMIM-PF<sub>6</sub> + water system.<sup>a</sup>

Electrical conductivity	Viscosity
Interaction parameters $\{ \text{BMIM}^+, \text{N}(\text{CF}_3\text{SO}_2)_2^- \} / \text{IL}^0, \text{IL}^0\text{b}$	
$\sigma^{00} = 23.2173$	$d^{10} = -0.236772$
$\sigma^{01} = 0.584842$	$d^{20} = 1.46357$
$d^{10} = 10.1056$	$b = 0.08$
$d^{11} = 0.0460024$	
$d^{20} = -30.8227$	
$d^{21} = -0.145853$	
$d^{30} = 19.8017$	
$d^{31} = 0.0412375$	
Interaction parameters $\{ \text{BMIM}^+, \text{N}(\text{CF}_3\text{SO}_2)_2^- \} / \text{IL}^0, \text{H}_2\text{O}$	
$\sigma^{00} = 84.6356$	
$\sigma^{01} = -2.73812$	
$d^{10} = 57.8554$	
$d^{11} = 2.12065$	
$d^{20} = -75.3990$	
$d^{21} = -3.15786$	
$d^{30} = 17.3421$	
$d^{31} = 1.11927$	
Limiting conductivity mixing-rule parameters	Solvent mixing-rule parameters
$k_{\text{N}(\text{CF}_3\text{SO}_2)_2^- / \text{IL}^0, \text{H}_2\text{O}}^{(0)} = -1.77920$	$k_{\text{IL}^0, \text{H}_2\text{O}}^{(0)} = -0.02892$
$g_{\text{N}(\text{CF}_3\text{SO}_2)_2^- / \text{IL}^0, \text{H}_2\text{O}}^{(0)} = 2.45507$	$g_{\text{IL}^0, \text{H}_2\text{O}}^{(0)} = 2.30494$
$k_{\text{BMIM}^+ / \text{IL}^0, \text{H}_2\text{O}}^{(0)} = -1.80427$	
$g_{\text{BMIM}^+ / \text{IL}^0, \text{H}_2\text{O}}^{(0)} = 0.139873$	
Literature data used for parameter determination: ranges of temperature and composition	
-10 to 100 °C in pure IL and 15–25 °C in IL-rich liquid phase	0–80 °C in pure IL and 20 °C in IL-rich liquid phase
$x_{\text{H}_2\text{O}} = 0 - 0.172$	$x_{\text{H}_2\text{O}} = 0 - 0.198$
References: 21, 24, 42–44	

<sup>a</sup> Models and parameters are described in [10] for electrical conductivity and in [11] for the viscosity.

<sup>b</sup> IL<sup>0</sup> stands for the undissociated BMIM.N(CF<sub>3</sub>SO<sub>2</sub>)<sub>2</sub> molecule, which has been treated as a solvent component.

dent on, among other variables, the identity and concentrations of the species that are present in a significant amount in the solution. The electrical conductivity and viscosity models described in Section 3, which were originally developed for mixed-solvent electrolyte systems [10,11], have been applied to analyze the experimental conductivity and viscosity data for the pure ionic liquid BMIM.N(CF<sub>3</sub>SO<sub>2</sub>)<sub>2</sub> and mixtures of this IL with water [21,24,42–44]. The results are presented in Figs. 10 and 11. The parameters for electrical conductivity and viscosity models that are necessary to reproduce these figures are given in Table 3. To emphasize the results at low water content in the mixtures of the ionic liquid with water, the conductivity and viscosity are presented as a function of the square root of the mole fraction of water (Fig. 10). The results show a good accuracy for the calculated electrical conductivity and viscosity. There is a rapid decrease in the viscosity of the ionic liquid in presence of even small levels of water. This decrease coincides with an increase in electrical conductivity (Fig. 10). The results illustrate the significant effect of the water content on transport properties, which may be the likely reason for disagreements

in the reported literature data as the atmospheric moisture can be rapidly absorbed by the ILs [42]. It should be noted that the electrical conductivity is an important measure of the degree of association in ionic solutions. The electrical conductivity results obtained in this study indicate that the speciation determined by the thermodynamic model is reasonable. This is further confirmed by the viscosity results, which are also highly dependent on the concentrations of ions and associated ion pairs.

## 7. Conclusions

Selected imidazolium-based ionic liquids and their mixtures with water and organic solvents have been analyzed using a comprehensive thermodynamic model and coupled transport property models. The ionic liquid has been treated as a dissociable species that is subject to chemical speciation, which is determined from available thermodynamic properties including activity coefficients, osmotic coefficients, enthalpies of mixing and solution, and heat capacities as well as phase equilibria. Transport properties, particularly electrical conductivities and viscosities, have been calculated based on the chemical speciation obtained from thermodynamic analysis. The accuracy of the thermodynamic model in representing the properties of ionic liquid systems has been verified by calculating vapor–liquid, liquid–liquid, and solid–liquid equilibria and by predicting the effects of chemical speciation, temperature, and concentrations on phase equilibria. The speciation results predicted by the thermodynamic model have been further used for calculating the electrical conductivity and viscosity of ionic liquid systems. The correct representation of electrical conductivity indicates that the thermodynamic speciation results are reasonable, thus providing a foundation for the simultaneous treatment of multiple properties in ionic liquid systems.

It should be noted that although the imidazolium-based ionic liquids are the only systems treated in the present study, the thermodynamic and transport property models described in this paper should be applicable, in general, to ionic liquids of other types. For example, the model's range of applicability has been demonstrated previously by accurate calculations of the melting temperatures of several nitrate salts [6]. A limitation of the current model lies in the use of the Helgeson–Kirkham–Flowers equation of state [15] for standard-state properties, which are based on the infinite dilution reference state in water, and, through a rigorous thermodynamic manipulation, are extended to non-aqueous or mixed solvents [6]. This standard-state property model is strongly affected by the temperature and pressure variations of pure water properties in the near-critical region. Thus, the application of the model to temperatures above ca. 300 °C may require using modified or alternative treatments of standard-state properties [8].

## Acknowledgements

This work was supported by Alcoa, Chevron, DuPont, Mitsubishi Chemical, Nippon Chemical, Rohm&Haas and Shell.

## References

- [1] A. Seidel (Ed.), Kirk-Othmer Encyclopaedia of Chemical Technology, vol. 26, 5th ed., John Wiley & Sons Inc., Hoboken, NJ, 2007, pp. 836–920.
- [2] Q. Dong, C.D. Muzny, A. Kazakov, V. Diky, J.W. Magee, J.A. Widegren, R.D. Chirico, K.N. Marsh, M. Frenkel, J. Chem. Eng. Data 52 (2007) 1151–1159.
- [3] A. Heintz, J. Chem. Thermodyn. 37 (2005) 525–535.
- [4] L.D. Simoni, Y. Lin, J.F. Brennecke, M.A. Stadtherr, Ind. Eng. Chem. Res. 47 (2008) 256–272.
- [5] C.C. Chen, L.D. Simoni, J.F. Brennecke, M.A. Stadtherr, Ind. Eng. Chem. Res. 47 (2008) 7081–7093.
- [6] P. Wang, A. Anderko, R.D. Young, Fluid Phase Equilib. 203 (2002) 141–176.
- [7] P. Wang, R.D. Springer, A. Anderko, R.D. Young, Fluid Phase Equilib. 222–223 (2004) 11–17.
- [8] P. Wang, A. Anderko, R.D. Springer, R.D. Young, J. Mol. Liquid 125 (2006) 37–44.

- [9] P. Wang, A. Anderko, R.D. Springer, J.J. Kosinski, M.M. Lencka, J. Geochem. Explor. 106 (2010) 219–225.
- [10] P. Wang, A. Anderko, R.D. Young, Ind. Eng. Chem. Res. 43 (2004) 8083–8092.
- [11] P. Wang, A. Anderko, R.D. Young, Fluid Phase Equilib. 226 (2004) 71–82.
- [12] K.S. Pitzer, J. Amer. Chem. Soc. 102 (1980) 2902–2906.
- [13] P. Wang, A. Anderko, Fluid Phase Equilib. 186 (2001) 103–122.
- [14] D.S. Abrams, J.M. Prausnitz, AIChE J. 21 (1975) 116–128.
- [15] H.C. Helgeson, D.H. Kirkham, G.C. Flowers, Am. J. Sci. 281 (1981) 1249–1516.
- [16] A. Anderko, M.M. Lencka, Ind. Eng. Chem. Res. 36 (1997) 1932–1943.
- [17] D.H. Zaitsau, G.J. Kabo, A.A. Strechan, Y.U. Paulechka, A. Tschersich, S.P. Verevkin, A. Heintz, J. Phys. Chem. A 110 (2006) 7303–7306.
- [18] Y.U. Paulechka, D.H. Zaitsau, G.J. Kabo, A.A. Strechan, Thermochim. Acta 439 (2005) 158–160.
- [19] M.J. Earle, J.M.S.S. Esperanca, M.A. Gilea, J.N. Canongia Lopes, L.P.N. Rebelo, J.W. Magee, K.R. Seddon, J.A. Widegren, Nature 439 (2006) 831–834.
- [20] J. Hunger, A. Stoppa, R. Buchner, G. Hefter, J. Phys. Chem. B 112 (2008) 12913–12919.
- [21] H. Tokuda, S. Tsuzuki, M. Hasan, K. Hayamizu, M. Watanabe, J. Phys. Chem. B 110 (2006) 19593–19600.
- [22] H. Weingärtner, Angew. Chem. Int. Ed. 47 (2008) 654–670.
- [23] H. Tokuda, K. Hayamizu, I. Kunikazu, M. Abu Bin Hasan Susan, M. Watanabe, J. Phys. Chem. B 108 (2004) 16593–16600.
- [24] H. Tokuda, K. Hayamizu, I. Kunikazu, M. Abu Bin Hasan Susan, M. Watanabe, J. Phys. Chem. B 109 (2005) 6103–6111.
- [25] P. Wang, A. Anderko, R.D. Springer, M.M. Lencka, Proceedings of the 17th International Symposium on Industrial Crystallization, Maastricht, The Netherlands, September 14–18, 2008, pp. 471–478.
- [26] D.S.H. Wong, J.P. Chen, J.M. Chang, C.H. Chou, Fluid Phase Equilib. 194–197 (2002) 1089–1095.
- [27] U. Domanska, A. Marciniak, J. Chem. Eng. Data 48 (2003) 451–456.
- [28] M. Krummen, P. Wasserscheid, J. Gmehling, J. Chem. Eng. Data 47 (2002) 1411–1417.
- [29] A. Heintz, L.M. Casas, I.A. Nesterov, V.N. Emel'yanenko, S.P. Verevkin, J. Chem. Eng. Data 50 (2005) 1510–1514.
- [30] J. Zhang, Q. Zhang, B. Qiao, Y. Deng, J. Chem. Eng. Data 52 (2007) 2277–2283.
- [31] R. Kato, J. Gmehling, Fluid Phase Equilib. 231 (2005) 38–43.
- [32] Ionic Liquids Database – (ILThermo) – NIST Standard Reference Database #147. <http://ilthermo.boulder.nist.gov/ILThermo/>.
- [33] M.G. Freire, L.M.N.B.F. Santos, A.M. Fernandes, J.A.P. Coutinho, I.M. Marrucho, Fluid Phase Equilib. 261 (2007) 449–454.
- [34] M. Doker, J. Gmehling, Fluid Phase Equilib. 227 (2005) 225–266.
- [35] S.P. Verevkin, J. Safarov, E. Bich, E. Hassel, A. Heintz, Fluid Phase Equilib. 236 (2005) 222–228.
- [36] S. Nebig, R. Boelts, J. Gmehling, Fluid Phase Equilib. 258 (2007) 168–178.
- [37] P.C. Ho, D.A. Palmer, R.E. Mesmer, J. Solution Chem. 23 (1994) 997–1018.
- [38] P.C. Ho, D.A. Palmer, J. Solution Chem. 24 (1995) 753–769.
- [39] J. Barthel, L. Iberl, J. Rossmäier, H.J. Gores, B. Kaukal, J. Solution Chem. 19 (1990) 321–337.
- [40] J.-F. Cote, G. Perron, J.E. Desnoyers, J. Solution Chem. 27 (1998) 707–718.
- [41] R.E. Mesmer, D.A. Palmer, J.M. Simonson, in: K.S. Pitzer (Ed.), Activity Coefficients in Electrolyte Solutions, 2nd ed., CRC Press, Boston, 1991, pp. 491–529.
- [42] J.A. Widegren, E.M. Saurer, K.N. Marsh, J.W. Magee, J. Chem. Thermodyn. 37 (2005) 569–575.
- [43] J.A. Widegren, A. Laesecke, J.W. Magee, Chem. Commun. (2005) 1610–1612.
- [44] K.R. Harris, M. Kanakubo, L.A. Woolf, J. Chem. Eng. Data 52 (2007) 1080–1085.
- [45] A.V. Blokhin, Y.U. Paulechka, A.A. Strechan, G.J. Kabo, J. Phys. Chem. B 112 (2008) 4357–4364.
- [46] Y. Qin, J.M. Prausnitz, Ind. Eng. Chem. Res. 45 (2006) 5518–5523.